DAΦNE TECHNICAL NOTE

INFN - LNF, Accelerator Division

Frascati, December 19, 1997

Note: **CD-10**

ANALYSIS OF THE DAΦNE BEAM POSITION MONITOR WITH A BOUNDARY ELEMENT METHOD

A. Stella

1. Introduction

Several different configurations of electrostatic beam position monitors (BPM) are installed all along the DAΦNE Main Rings (MR) to measure the closed orbit distortion.

Each monitor consists of button pickup electrodes located symmetrically around the vacuum chamber.

In order to reconstruct accurately the beam transverse position, a sensitivity analysis of each type of BPM installed in the MR has been performed to recover the non linearity of the transfer function.

This note deals with the finite element numerical method applied to characterize the Main Rings BPM, results and comparisons between numerical and experimental data are reported.

2. BPM calibration

A beam pickup can be thought of as a discontinuity in the vacuum chamber of the storage ring, which interrupts and diverts into a measuring device a portion of the wall image-current induced by the beam.

If the beam is displaced from the center of the vacuum chamber the magnetic and electric fields are modified accordingly, so we can measure the beam position through the relative amplitudes of the induced signal on each button. Such signals depend in a non-linear way from the beam position, so it is important, in order to reconstruct accurately the beam position, to develop an algorithm to process the measured data.

In DAΦNE we use a non linear fit of two dimensionless quantities U,V derived from the charge Q induced on electrodes:

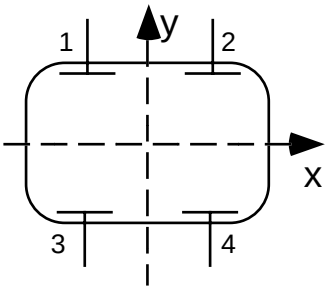

$$U = \frac{1}{2}\left[\left(\frac{Q_2 - Q_3}{Q_2 + Q_3}\right) + \left(\frac{Q_4 - Q_1}{Q_4 + Q_1}\right)\right]$$

$$V = \frac{1}{2}\left[\left(\frac{Q_2 - Q_3}{Q_2 + Q_3}\right) - \left(\frac{Q_4 - Q_1}{Q_4 + Q_1}\right)\right]$$

Figure 1: Schematic of a BPM and (U,V) definition.

The beam position (x_0,y_0) is derived, through a recursive algorithm, with the following implicit polynomial functions [6]:

$$\begin{aligned} x_0 &= K_x(x_0,y_0)\cdot U \\ y_0 &= K_y(x_0,y_0)\cdot V \end{aligned} \tag{1}$$

where:

$$\begin{aligned} K_x(x_0,y_0) &= a_0 + a_1 y_0^2 + a_2 y_0^4 + a_3 x_0^2 + a_4 x_0^2 y_0^2 + a_5 x_0^4 \\ K_y(x_0,y_0) &= b_0 + b_1 y_0^2 + b_2 y_0^4 + b_3 x_0^2 + b_4 x_0^2 y_0^2 + b_5 x_0^4 \end{aligned} \tag{1a}$$

A Fortran routine, performing a least squares fit, has been developed in order to deduce the unknown coefficients a_i and b_i starting from $\{x_0,y_0,U,V\}$ values obtained from the calibration data. Such coefficients allow, during machine operation, to reconstruct accurately the transverse beam position starting from the measured values U,V.

3. A numerical method to characterize BPM

In order to determine the proper fitting functions, calibration of each monitor is required.

For the DAΦNE BPM two methods were implemented to deduce the quantities U,V for a given beam position. One method is based on the numerical solution of the two dimensional electrostatic problem defined in the closed boundary surrounded by the beam pipe, another method consists of experimental measurements on a prototype.

In this note more emphasis is given to the former, which represents a fast and reliable way to obtain calibration data about any BPM. Details about the latter method can be found in [6].

It can be shown that the determination of the signal induced by the beam on the button electrodes can be reduced, in case of relativistic beams, to a two dimensional electrostatic problem whose unknown is the induced charge on the boundary [1] [7].

For this reason we derive, for a given beam position, the induced charge Q_i from the solution of an electrostatic problem defined in a two dimensional region Ω closed by the boundary Γ (the beam pipe), containing the charge density $\rho(x,y)$ that represents the beam (Fig. 2).

The electrostatic field as a function of (x,y) is given by a scalar potential $\phi(x,y)$ as follows:

$$\mathbf{E}(x,y) = -\nabla\phi(x,y) \tag{2}$$

where $\phi(x,y)$ satisfies over the surface Ω the Poisson equation:

$$\nabla^2\phi(x,y) = -\frac{\rho(x,y)}{\varepsilon_0} \tag{3}$$

If we assume a perfect conducting material for the vacuum chamber, the solution $\phi(x,y)$ must satisfy the following Dirichlet boundary conditions:

$$\phi(\mathbf{r}) = 0 \qquad \text{if} \qquad \mathbf{r} \equiv (x,y) \in \Gamma \tag{4}$$

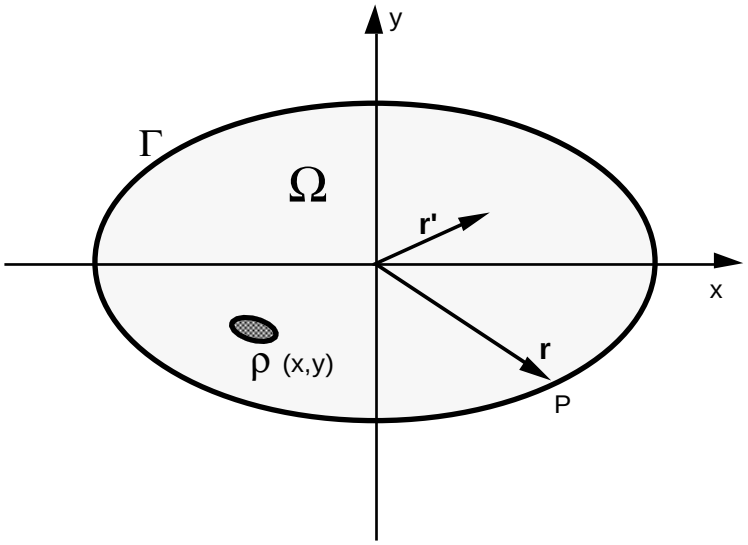

Figure 2: Schematic of the electrostatic problem, Γ is the vacuum chamber boundary, the charge density ρ represents the beam.

Applying Green's theorem the differential equation (3) can be expressed by the corresponding integral equation. The potential at a fixed point P with coordinates **r**=(*x*,*y*) on the boundary Γ can be expressed by a surface integral plus a curvilinear integral over Γ, as:

$$\frac{1}{2}\phi(\mathbf{r}) = \frac{1}{2\pi\varepsilon_0}\iint_{\Omega}\rho(\mathbf{r}')\ln\frac{1}{|\mathbf{r}-\mathbf{r}'|}d\Omega + \frac{1}{2\pi}\oint_{\Gamma}\left[\frac{\partial\phi}{\partial n}\ln\frac{1}{|\mathbf{r}-\mathbf{r}'|} - \phi(\mathbf{r}')\ln\frac{1}{|\mathbf{r}-\mathbf{r}'|}\right]d\Gamma$$

the surface integral represents the contribution of the sources inside Ω, while the surface integral term represents the contributions to $\phi(\mathbf{r})$ of the sources on the boundary Γ [4] [5].
To deduce the induced charge on the boundary wall consider the point P(**r**) along the curve Γ, we have the following situation:

$$\frac{\partial\phi(\mathbf{r})}{\partial n} = \nabla\phi\cdot\mathbf{n} = -\mathbf{E}\cdot\mathbf{n} = \frac{\sigma(\mathbf{r})}{\varepsilon_0} \quad \text{with} \quad \mathbf{r}\in\Gamma$$

so the equation to solve reduces to:

$$0 = \int_{\Omega}\rho(\mathbf{r}')\ln\frac{1}{|\mathbf{r}-\mathbf{r}'|}d\Omega + \int_{\Gamma}\sigma(\mathbf{r}')\ln\frac{1}{|\mathbf{r}-\mathbf{r}'|}d\Gamma \tag{5}$$

where $\sigma(\mathbf{r})$ is our unknown, i.e. the charge density induced by the beam on the surface of the beam pipe. At this point the charge Q_i along the generic button electrodes, that we assume to be flush with the wall, is:

$$Q_i = \int_{l_i}\sigma(\mathbf{r}')L(\mathbf{r}')d\Gamma \tag{6}$$

where $L(\mathbf{r}')$ is the length of the button electrodes in the longitudinal direction and l_i is the button diameter.

The integral equation (5) can not be solved analytically in every case, so a boundary element numerical method (BEM) has been implemented [2]. BEM is based on the previous integral formulation of the electromagnetic problem [3][4]. It allows a finite elements solution of a problem that has been reduced to deal with the boundary Γ rather than the whole region of definition Ω, in other words it reduces the dimensions of the problem by one.

Discretization of (5) allows to transform the integral equation into a set of algebraic equations. The boundary Γ and the surface Ω are divided respectively in M and M_1 small elements (boundary elements) and ρ_i and σ_i are the charge density of the i-th element. For the j-th boundary element we can write:

$$\phi(\mathbf{r}_j) = 0 = \sum_{k=1}^{M} \int_{\Gamma_k} \sigma_k(\mathbf{r}_i) \ln \frac{1}{|\mathbf{r}_i - \mathbf{r}_j|} dr_i + \sum_{k=1}^{M_1} \int_{\Omega_k} \rho_k(\mathbf{r}_i) \ln \frac{1}{|\mathbf{r}_i - \mathbf{r}_j|} dr_i$$

At this point, under the following hypothesis:

- the charge density $\rho(x,y)$ that represents the beam is concentrated in a single point $\mathbf{r}_0=(x_0,y_0)$ or, in other words, the beam has negligible transverse size regard to the vacuum chamber dimension.
- the unknown charge density $\sigma(x,y)$ induced from the beam on the pipe wall is constant over each boundary element ("constant elements");

the integral equation (for every fixed *j*) reduces to:

$$\sum_{k=1}^{M} \sigma_k \int_{\Gamma_i} \ln \frac{1}{|\mathbf{r}_i - \mathbf{r}_j|} dr_i + \int_{\Omega} \delta(\mathbf{r}_i - \mathbf{r}_0) \ln \frac{1}{|\mathbf{r}_i - \mathbf{r}_j|} dr_i = 0 \qquad (7)$$

By introducing the [**G**] matrix, with MxM elements:

$$G_{ji} = \int_{\Gamma_i} \ln \frac{1}{|\mathbf{r}_i - \mathbf{r}_j|} dr_i \qquad (8)$$

and the column vector **B** with elements B_j:

$$B_j = \ln \frac{1}{|\mathbf{r}_0 - \mathbf{r}_j|} \qquad (9)$$

it is possible to use a matrix notation to represent eq.(7):

$$[\mathbf{G}]\sigma + \mathbf{B} = \mathbf{0} \qquad (10)$$

where σ is the unknown column vector whose elements are the induced charge density on each boundary element, supposed to be concentrated in the center of the element:

$$\sigma_i = \sigma(\mathbf{r}_j) \qquad j = 1.....M \qquad (10b)$$

With the above considerations the integral equation (5) that describes the electrostatic problem has been transformed into a set of M algebraic equations (10).

By inverting the matrix [**G**] the induced charge distribution σ over the boundary elements, and hence on every button electrode, is obtained:

$$\sigma = -[\mathbf{G}]^{-1} \cdot \mathbf{B} \tag{11}$$

An appropriate software has been developed to calculate the numerical solution for σ solving eq.(10). For a given geometry of the beam pipe, knowing the position of the beam (x_0,y_0) and the electrodes location over the boundary, it is possible to deduce the charge induced on every button and hence the two quantities (U,V).

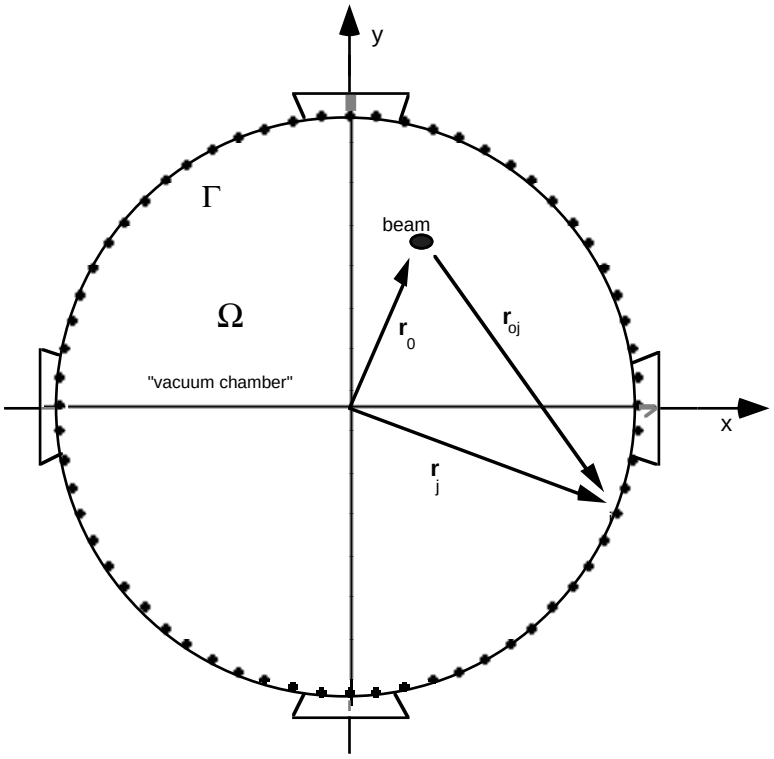

Figure 3: Beam pipe section and boundary elements division.

4. Results

In this chapter we report the results obtained for three specific configurations.

To check the reliability of the finite element code it is useful to compare the results with the experimental measurements performed on each BPM.

We have measured the output signals induced on each electrode with the method based on a coaxial wire put along the beam tube [6] [7]. The BPM block is mounted on a fixed stage and a wire strung coaxially along the pipe simulates the beam field with a RF signal generated by a network analyzer. The wire can be moved transversely inside the monitor by a movable arm. The BPM electrodes are connected to a multiplexer whose output goes into the network analyzer port A, the voltage (normalized to the input power) at twice the Main Rings RF is measured and stored for every position of the moveable arm. A Macintosh computer controls via GPIB all the system parts, so that the measurement is completely automatic.

To guarantee accuracy to the BEM numerical solutions it is crucial to maximize the number of finite elements used to subdivide the boundary. Since also the computing time grows with the number of finite elements a compromise must be found.

The simplest way is to increase iteratively the total number of elements in each single case, up to an effective convergence of the results.

As a general rule we adopted a more dense mesh in the vicinity of button electrodes, in order to have a better approximation where it is needed, so that the length of each boundary elements vary between 1 mm and 3.5 mm.

We get accurate solutions with computing times below 1 hour on a Macintosh IIci (for calibration maps of 100 points). In our case making use of constant elements that still maintain the actual shape of the boundary was the key to find accurate solutions in a reasonable time and with a low computing effort.

The cross sectional view of the simple round position monitor is shown in Fig. 4, the position map obtained is in Fig. 5. In this case the boundary was divided in 48 elements, the position sensitivity, i.e. the two coefficients a_0 e b_0 in eq.(1b), are correct within an error of ~1% with respect to the measured value (Tab. 1).

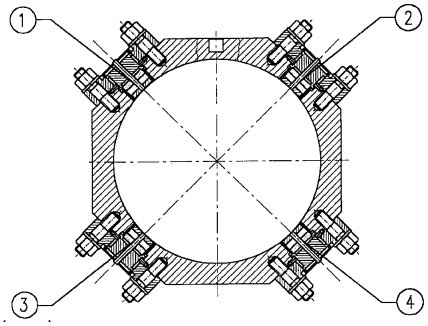

Figure 4: Cross sectional view of the Round BPM (radius 44 mm).

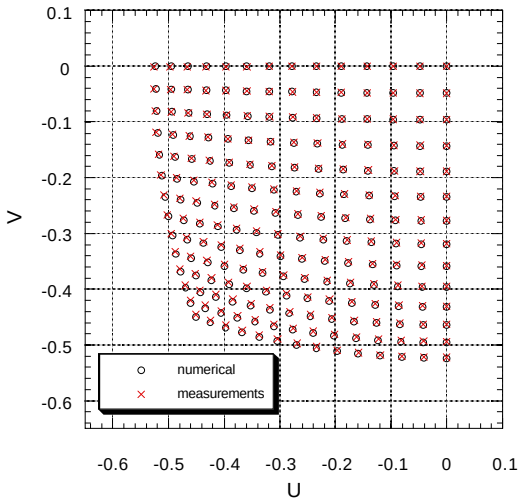

Figure 5: Calibration map for the Round BPM, comparison between numerical and experimental results. Distance between dots is 1 mm.

Table 1: Coefficients a_0 and b_0 for the Round BPM deduced with different methods

solution type	$a_0=b_0$	*error %*
analytical [7]	31.38 mm	-1 %
numerical	31.48 mm	-0.7 %
measurements	31.70 mm	-----

For the BPM with rectangular cross section (Fig. 6) the boundary was divided in 60 elements; experimental and numerical results are reported together in the calibration map for a 30 mm x 30 mm zone around the center of the vacuum chamber (Fig. 7 and Tab. 2).

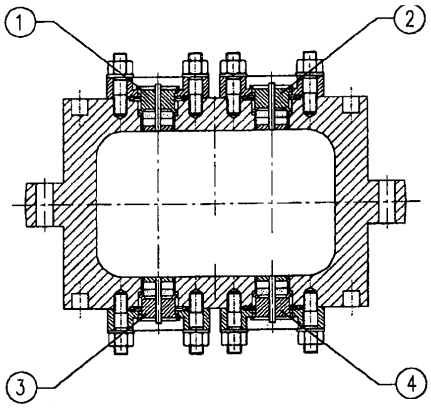

Figure 6: cross sectional view of the Rect BPM (88mm x 42mm).

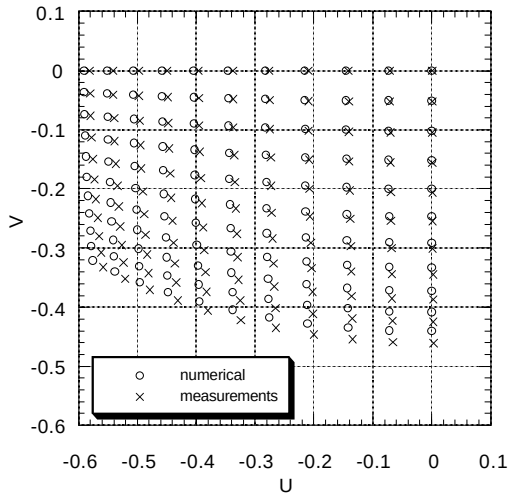

Figure 7: calibration map for the Rect BPM, comparison between numerical and experimental results. Distance between dots is 1.5mm.

Table 2: coefficients a_0 and b_0 for the Rect BPM deduced with different methods

	numerical	measurements	*error %*
a_0	20.74 mm	21.32 mm	-2.7 %
b_0	29.37 mm	29.27 mm	0.34 %

The BPM in Fig.8 is installed in the DAΦNE Interaction Regions (IR) In this case the boundary has been divided in 80 small elements. Results are compared in Fig. 9 and Tab. 3 and are referred to button electrodes n.1-2-5-6, and show good agreement.

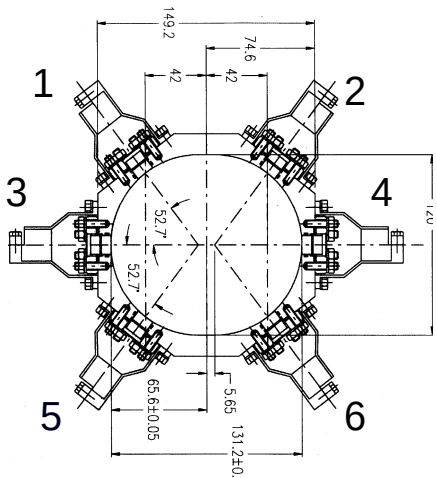

Figure 8: cross sectional view of the IR BPM (131mm x 60mm).

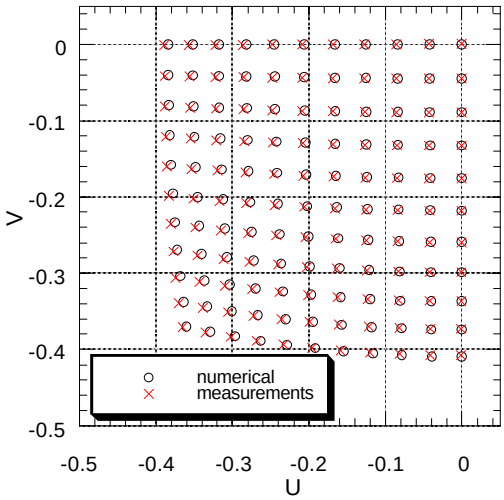

Figure 9: calibration map (sector) for the IR BPM, comparison between numerical and experimental results.Distance between dots is 2 mm.

Table 3: coefficients a_0 and b_0 for the IR BPM deduced with different methods

	numerical	measurements	*error %*
a_0	47.33 mm	46.71 mm	1.3 %
b_0	44.64 mm	44.97 mm	-0.7 %

References

[1] J.H. Cuperus, "Monitoring of particle beams at high frequencies", Nuclear Instruments and Methods, 145 (1977) pp.219.

[2] T. Shintake et al., " Sensitivity calculation of beam position monitor", Nuclear Instruments and Methods in Physics Research A254 (1987) pp146-150.

[3] P. Zhou, "Numerical Analysis of Electromagnetic Fields", ed.Springer-Verlag.

[4] N. Morita et al., "Integral Equation Methods for Electromagnetics", ed.Artech House (1987).

[5] J.D. Jackson, "Classical Electrodynamics", ed.J.Wiley (New York).

[6] A. Ghigo, F. Sannibale, M. Serio, C. Vaccarezza: "The DAΦNE Beam Position Monitors", Proc. Beam Instrumentation Workshop , Argonne 1996.

[7] R. Shafer, "Beam Position Monitoring" AIP Conf.Proc. 105 (1992).